

Gravitational Waves from Compact Objects Accreting onto Active Galactic Nuclei

Jeremy Schnittman, Günter Sigl, and Alessandra Buonanno

Citation: [AIP Conference Proceedings](#) **873**, 437 (2006); doi: 10.1063/1.2405081

View online: <http://dx.doi.org/10.1063/1.2405081>

View Table of Contents:

<http://scitation.aip.org/content/aip/proceeding/aipcp/873?ver=pdfcov>

Published by the [AIP Publishing](#)

Articles you may be interested in

[Cluster Magnetic Fields from Active Galactic Nuclei](#)

AIP Conf. Proc. **1201**, 346 (2009); 10.1063/1.3293073

[Gravitational Wave Sources from New Physics](#)

AIP Conf. Proc. **873**, 30 (2006); 10.1063/1.2405019

[Spherical Accretion in Nearby Weakly Active Galactic Nuclei](#)

AIP Conf. Proc. **801**, 216 (2005); 10.1063/1.2141868

[Gravitational wave emission from matter accretion onto a Schwarzschild black hole](#)

AIP Conf. Proc. **751**, 221 (2005); 10.1063/1.1891558

[Gravitational wave background from coalescing compact stars in eccentric orbits](#)

AIP Conf. Proc. **586**, 787 (2001); 10.1063/1.1419657

Gravitational Waves from Compact Objects Accreting onto Active Galactic Nuclei

Jeremy Schnittman*, Günter Sigl[†] and Alessandra Buonanno*

**Physics Department, University of Maryland, College Park, MD 20742*

*[†]AstroParticules et Cosmologie, 11 place Marcelin Berthelot, F-75005 Paris, France
Institut d'Astrophysique de Paris, 98bis Boulevard Arago, 75014 Paris, France*

Abstract. We consider a model in which massive stars form in a self-gravitating accretion disk around an active galactic nucleus. These stars may evolve and collapse to form compact objects on a time scale shorter than the accretion time, thus producing an important family of sources for LISA. Assuming the compact object formation/inspiral rate is proportional to the steady-state gas accretion rate, we use the observed extra-galactic X-ray luminosity function to estimate expected event rates and signal strengths. We find that these sources will produce a continuous low-frequency background detectable by LISA if more than $\gtrsim 1\%$ of the accreted matter is in the form of compact objects. For compact objects with $m \gtrsim 10M_{\odot}$, the last stages of the inspiral events should be resolvable above a few mHz, at a rate of $\sim 10 - 100$ per year.

Keywords: gravitational waves, AGN

PACS: PACS: 04.80.Nn, 98.54.Cm, 95.55.Ym

INTRODUCTION

One of the major challenges that will face gravitational wave (GW) astronomers is the successful discrimination between instrumental noise, stochastic GW backgrounds, and individual, resolvable GW sources. For example, the population of galactic white dwarf binaries in close orbits will provide a major contribution to the LISA noise curve in the $0.1 - 1$ mHz band [1]. At the same time, this confusion “noise” can also be treated as a signal, and its shape and amplitude will provide important information about the distribution and properties of white dwarf binaries in the galaxy.

It has recently been proposed that, in the self-gravitating accretion disks of active galactic nuclei (AGN), massive stars could form and evolve, eventually collapsing into compact objects and merging with the central black hole [2, 3]. At different stages in the inspiral evolution, this population will contribute to the GW background confusion or alternatively produce individual, resolvable chirp signals. It is therefore a matter of theoretical and practical interest to understand the nature of such a population.

In this paper we derive a relationship between the observable electro-magnetic (EM) emission and the predicted GW emission from AGN, following the procedures and summarizing the results outlined in our longer paper [4]. In particular, we use the hard X-ray luminosity function of Ueda et al. [5] to infer the accretion history of supermassive black holes (SMBHs) out to redshifts of $z \sim 3$. Then we assume a few simple scaling factors, such as the average (Eddington-scaled) accretion rate and the efficiency of converting accretion energy to X-rays, and derive the GW spectrum that might be seen by LISA.

CP873, *Laser Interferometer Space Antenna—6th International LISA Symposium*,

edited by S. M. Merkowitz and J. C. Livas

© 2006 American Institute of Physics 978-0-7354-0372-7/06/\$23.00

437

TABLE 1. Glossary of dimensionless parameters, with allowable and preferred values

symbol	min	max	preferred	description
f_{acc}	0	1	1	fraction of SMBH mass due to accreted gas
f_{co}	0	1	0.01	fraction of SMBH mass due to accreted compact objects
f_{X}	0	1	0.03	fraction of EM radiation in X-rays
f_{Edd}	0	$\gtrsim 1$	0.1	typical fraction of Eddington luminosity/accretion rate
η_{em}	0	1	0.2	efficiency of converting accreting gas to EM radiation
η_{gw}	0	1	0.2	efficiency of converting compact objects to GW radiation

Depending on the specific model parameters, we find this background could be an important class of LISA sources, similar in strength and event rates to extreme mass-ratio inspirals from captured compact objects [6]. As in those sources, here too it is a matter of preference as to whether the background should be thought of as signal or noise. But for higher masses (perhaps as large as $m \simeq 10^5 M_{\odot}$ [2]), disk-embedded compact objects should produce individual, resolvable inspiral events with high signal-to-noise over a wide band of frequencies.

THE HARD X-RAY LUMINOSITY FUNCTION OF AGN

We begin with a short discussion of notation. The results derived below include a number of dimensionless parameters, most of which can take values between 0 and 1. We divide these parameters into two general classes: efficiencies and fractions. Efficiencies, denoted by η , are believed to be determined by more fundamental physics, and typically have more stringent lower- and upper-limits. Fractions, denoted by f , are more model-dependent parameters and less-well known than the efficiency parameters, and thus have a larger range of acceptable values. A summary of these model parameters appears in Table 1.

A growing consensus has been forming that SMBHs grow almost exclusively by accretion, suggesting $f_{\text{acc}} \simeq 1$ (see, e.g. [7]). A corollary of this assumption is that most AGN should be rapidly spinning, with dimensionless spin parameters of $a/M \simeq 0.9 - 0.998$, giving EM efficiencies for a radiative disk of $\eta_{\text{em}} \simeq 0.15 - 0.32$ [8]. Similarly, assuming the compact objects are on circular, adiabatic orbits, we set $\eta_{\text{gw}} = \eta_{\text{em}}$, ignoring any EM or GW emission from the plunging region.

We write the X-ray luminosity L_{X} as a fraction f_{X} of the bolometric luminosity, which in turn is a fraction f_{Edd} of the Eddington luminosity L_{Edd} :

$$L_{\text{X}} = f_{\text{X}} f_{\text{Edd}} L_{\text{Edd}}(M) = f_{\text{X}} \eta_{\text{em}} \dot{M}_{\text{acc}} c^2. \quad (1)$$

The Eddington limit is a function only of the SMBH mass: $L_{\text{Edd}}(M) = 1.3 \times 10^{38} (M/M_{\odot})$. Over the range of redshifts and luminosities we are probing, typical accretion rates are estimated to be $f_{\text{Edd}} \sim 0.1$, but could conceivably be even greater than unity [9]. Since the energy density in the cosmic infrared background (also dominated by AGN) is about 30 times greater than the X-ray background, we set $f_{\text{X}} = 0.03$ [10]. Lastly, the parameter f_{co} is the fraction of total mass accreted in the

form of compact objects. Since the astrophysical mechanisms that actually determine this fraction are not yet well understood, we set it to a conservative value of 0.01. If it were much higher, the disk would be entirely fragmented and thus not efficiently emit EM radiation. And as we will see below, a value much below 0.01 would result in a GW signal undetectable by LISA.

We approximate the intrinsic (i.e. directly produced by the accretion process, and before reprocessing and/or partial absorption within the host galaxy) X-ray luminosity function per comoving volume after Ref. [5], roughly giving a broken power-law distribution with higher average luminosities at higher redshift. The fiducial values for the model parameters and the observed range of luminosities correspond to SMBH masses in the range $10^6 M_\odot \lesssim M \lesssim 10^{10} M_\odot$, consistent with the masses inferred from observations of velocity dispersions.

THE GRAVITATIONAL WAVE SPECTRUM

We begin by considering the inspiral of a single compact object of mass m onto a SMBH of mass $M \gg m$ and specific angular momentum a . Using geometrized units such that $G = c = 1$, a particle on a circular, equatorial orbit around a Kerr black hole has an orbital frequency (as measured by an observer at infinity) of

$$f_{\text{orb}}(r) = \frac{\sqrt{M}}{2\pi(r^{3/2} + a\sqrt{M})} \quad (2)$$

and specific energy

$$\frac{E(r)}{m} = \frac{r^2 - 2Mr + a\sqrt{Mr}}{r(r^2 - 3Mr + 2a\sqrt{Mr})^{1/2}}. \quad (3)$$

Thus the total energy emitted in gravitational waves down to a radius r is $E_{\text{gw}}(r) = m - E(r)$. The GW energy emitted between frequency f and $f + df$ for such an event is

$$\frac{dE_{\text{gw}}}{df} = \frac{dE_{\text{gw}}}{dr} \left(\frac{df}{dr} \right)^{-1}. \quad (4)$$

Here, we restrict the GW emission to the quadrupole formula for circular geodesic orbits, thus we consider only GW frequencies at twice the orbital frequencies ($f = 2f_{\text{orb}}$).

We will generally want to restrict equation (4) to a range of frequencies $f_{\text{min}} \leq f \leq f_{\text{max}}$, where f_{min} is determined by the LISA sensitivity and f_{max} is the GW frequency at the inner-most stable circular orbit (ISCO). The ISCO frequency in turn is determined solely by the SMBH mass and spin, giving $f_{\text{max}} \simeq 4 - 30$ mHz for $M = 10^6 M_\odot$. In Figure 1 we show the characteristic strain spectrum for a single inspiral event for a range of black hole masses and spins.

Integrated over redshift z , the observed GW energy density per logarithmic frequency is given by (e.g. [11])

$$\frac{d\rho_{\text{gw}}(f)}{d\ln f} = \int_0^\infty dz \frac{R(z)}{1+z} \left| \frac{dt}{dz} \right| \frac{dE_{\text{gw}}}{d\ln f_z}(f_z), \quad (5)$$

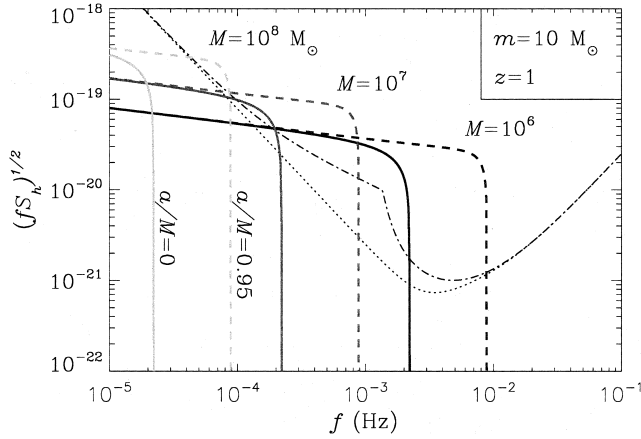


FIGURE 1. Characteristic GW strain amplitudes for individual inspiral events, where a black hole with $m = 10M_\odot$ merges with a SMBH of mass $M = 10^6, 10^7, 10^8 M_\odot$ at a redshift of $z = 1$. For each value of M , we show the spectra for two spin values, $a/M = 0$ (solid) and 0.95 (dashed). The dot-dashed and dotted lines are the sky-averaged LISA noise curves with and without the contributions from galactic binaries, respectively.

where $f_z \equiv (1+z)f$, and $R(z)$ is the rate of inspiral events per comoving volume. Cosmology enters with the term $|dt/dz| = [(1+z)H(z)]^{-1}$, where for a flat geometry,

$$H(z) = H_0 [\Omega_M(1+z)^3 + \Omega_\Lambda]^{1/2}. \quad (6)$$

Throughout this paper we will assume a standard Λ CDM universe with $\Omega_M = 0.3$, $\Omega_\Lambda = 0.7$, and $H_0 = 72 \text{ km s}^{-1} \text{ Mpc}^{-1}$.

The event rate for a single AGN is simply the X-ray luminosity divided by the total X-ray energy emitted between inspiral events: $E_X = E_{\text{gw}} f_X / f_{\text{co}}$. Integrating over the luminosity distribution function, we get

$$R(z) = \frac{f_{\text{co}}}{f_X} \int dL_X \frac{dn(L_X, z)}{d \ln L_X} \frac{1}{E_{\text{gw}}}, \quad (7)$$

where $dn(L_X, z)/d \ln L_X$ is the intrinsic luminosity distribution function in units of Mpc^{-3} . Combining equations (5) and (7), the total (time-averaged) gravitational wave spectrum is

$$\frac{d\rho_{\text{gw}}(f)}{d \ln f} = \frac{f_{\text{co}}}{f_X} \int_0^\infty \left| \frac{dt}{dz} \right| \frac{dz}{1+z} \int_{L_{\text{min}}}^{L_{\text{max}}} dL_X \frac{dn}{d \ln L_X} \frac{1}{E_{\text{gw}}} \frac{dE_{\text{gw}}}{d \ln f_z}(f_z). \quad (8)$$

The GW spectrum $E_{\text{gw}}(f)$ from each individual AGN is a function of the SMBH mass, which in turn is determined by the X-ray luminosity through equation (1). Note that the integrated spectrum is independent of m , as long as m is small enough so that the inspiral waveform cannot be individually resolved. One measure of this resolvability is the *duty cycle*, described in the next section.

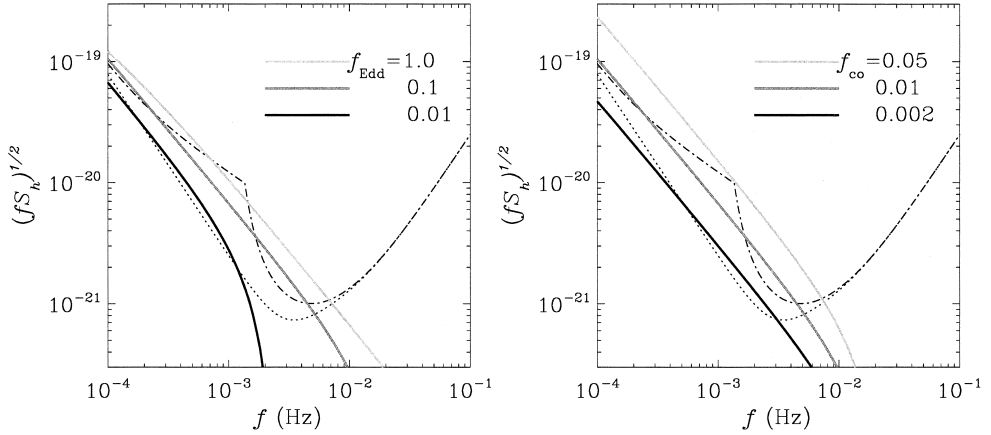


FIGURE 2. Dependence of the GW background on the model parameters f_{Edd} (left) and f_{co} (right). The fiducial values for the model give a background signal comparable to the LISA noise curve, including unresolved galactic white dwarf binaries.

Following Refs. [6, 12], we will want to compare directly the background defined in equation (8) to the spectral density of the detector noise $S_n(f)$, which has units of inverse frequency. In this case, $\sqrt{fS_n(f)}$ will be a dimensionless strain. Averaging over the entire sky, weighted by the LISA antenna pattern, gives

$$S_h(f) = \frac{4}{\pi} \frac{1}{f^3} \frac{d\rho_{\text{gw}}(f)}{d\ln f}. \quad (9)$$

Throughout the paper we use the so-called sky and detector averaged instrumental spectral density for LISA, augmented by the white-dwarf galactic confusion noise, as given in [6].

In Figure 2 we plot the nominal GW background from equation (8) with the model parameters listed in Table 1. Also shown are the effects of varying the accretion rate f_{Edd} (Fig. 2a) and the fraction of accreted mass in compact objects f_{co} (Fig. 2b). By increasing f_{Edd} , the effect is to reduce the AGN mass inferred from equation (1) and thus increase the GW frequency of the signal, shifting the curves to the right. From the leading term in equation (8), it is clear that the total GW power is simply proportional to f_{co} , so increasing this parameter linearly increases the total amplitude of the GW spectrum.

EVENT RATES AND RESOLVABLE SIGNALS

The GW spectra calculated from equation (8) represent the *time-averaged* signal from all the AGN in the universe, but at any single time, there may only be a few sources that are emitting at a given frequency. This can be seen from comparing Figures 1 and 2: while the signal-to-noise ratio of a single inspiral can be very large around 1 – 10 mHz,

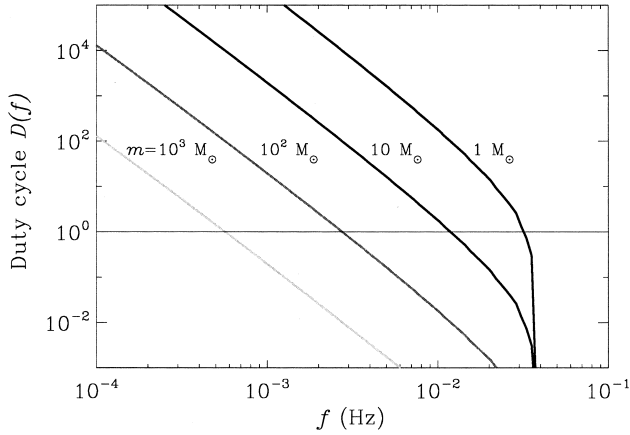


FIGURE 3. Duty cycle $D(f)$ for the nominal parameter values and a range of compact object masses m . When $D(f) \lesssim 1$, the inspiral signals should be individually resolvable.

a relatively small fraction of the inspiral time is spent in that band, significantly reducing the time-averaged strain amplitude.

One way of estimating the number of individual signals at a given frequency is by calculating the duty cycle $D(f)$:

$$D(f) = \frac{f_{\text{co}}}{f_X m \eta_{\text{gw}}} \int dz \frac{dV}{dz} \int_{L_{\text{min}}}^{L_{\text{max}}} dL_X \frac{dn}{d \ln L_X} t_{\text{coh}}(f_z), \quad (10)$$

where the cosmological volume element is $dV/dz = 4\pi r^2(z)/H(z)$ and the “coherence time” $t_{\text{coh}}(f)$ is approximated by the Newtonian limit of the radiation reaction formula (e.g. [13]):

$$t_{\text{coh}}(f) \equiv \frac{f}{df/dt} \simeq \frac{5}{144} m^{-1} M^{-2/3} (\pi f)^{-8/3}. \quad (11)$$

In Figure 3 we show the duty cycle for the fiducial model parameters and a range of compact object masses m . The sharp cutoff around 40 mHz is not physical, but rather due to the somewhat artificial low-end cutoff in the luminosity function, corresponding to a minimum value for M and thus maximum attainable frequency. Note that $D(f)$ is proportional to m^{-2} , since smaller m means more compact objects, and also slower inspiral rates, thus each source spends more time around a given f .

It is important to understand that $D(f)$ represents the total number of sources in the observable universe, not all of which would be individually resolvable with LISA. To estimate the subtractable portion of the signal, we integrate the total signal-to-noise ratio (SNR) for a three-year mission lifetime (see, e.g., [12]). For a given m , M , and source distance d , we can calculate the minimum frequency above which the source would be detectable with SNR above a certain threshold (here we use 15). Any contribution to equation (8) above that frequency is ignored, resulting in an unresolvable GW spectrum,

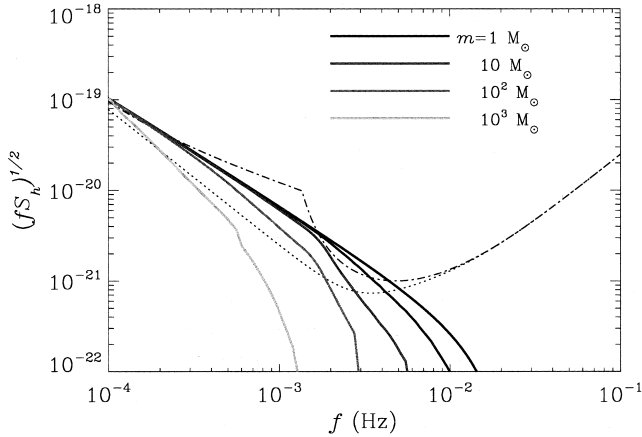


FIGURE 4. The fiducial time-averaged signal (*top curve*), along with the unresolvable portions of the GW spectra, after subtracting out individual events with integrated SNR above a threshold of 15.

plotted in Figure 4. As expected, with increasing m , more inspiral events are detectable and the remaining background confusion noise is diminished.

ACKNOWLEDGMENTS

We thank Curt Cutler and Joe Silk for useful discussions.

REFERENCES

1. P.L. Bender and D. Hils, *Classical Quantum Gravity* **14**, 1439 (1997).
2. J. Goodman and J. C. Tan, *Astrophys. J.* **608**, 108 (2004).
3. Y. Levin, *Mon. Not. Royal Acad. Sci.* submitted (2006) [arXiv:astro-ph/0603583].
4. G. Sigl, J. D. Schnittman, and A. Buonanno, *Phys. Rev. D* submitted (2006).
5. Y. Ueda, M. Akiyama, K. Ohta, and T. Miyaji, *Astrophys. J.* **598**, 886 (2003).
6. L. Barrack and C. Cutler, *Phys. Rev. D* **70**, 122002 (2004).
7. Q. j. Yu and S. Tremaine, *Mon. Not. Roy. Astron. Soc.* **335**, 965 (2002).
8. K. S. Thorne, *Astrophys. J.* **191**, 507 (1974).
9. A. Marconi, G. Risaliti, R. Gilli, L. K. Hunt, R. Maiolino and M. Salvati, *Mon. Not. Roy. Astron. Soc.* **351**, 169 (2004).
10. M. T. Ressler and M. S. Turner, *Comments Astrophys.* **14**, 323 (1990).
11. E. S. Phinney, [astro-ph/0108028].
12. L. S. Finn and K. S. Thorne, *Phys. Rev. D* **62**, 124021 (2000).
13. P. C. Peters, *Phys. Rev.* **136**, B1224 (1964).